



# Dynamic Response Analysis of Substation Steel Frame Strengthened with BRB

Feng Dong<sup>1,2</sup>, Jianan Wang<sup>2\*</sup>, Zhenchao Teng<sup>2,3</sup>, Jiahao Zhang<sup>2</sup>, Fengyuan Fu<sup>2</sup>

<sup>1</sup>Hulun Buir Branch of Daqing Oilfield Co. Ltd, Daqing, Heilongjiang, 163712, China

<sup>2</sup>College of Civil Engineering & Architecture, Northeast Petroleum University, Daqing, Heilongjiang, 163318, China

<sup>3</sup>Key Laboratory of Disaster Prevention, Mitigation and Protection Engineering in Heilongjiang Province, Daqing Heilongjiang 163318, China

\*Corresponding author's e-mail: wang\_jianana@126.com

**Abstract.** To investigate the dynamic response of the frame structure of the skid-mounted substations with electronic control reinforced by buckling-restrained braces (BRBs) under high-intensity earthquake and wind loads, the study utilized the Plastic (Wen) connection element in SAP2000 finite element software to simulate the behavior of the BRB structure, and the response spectrum and nonlinear time history analyses were conducted. These analyses demonstrate that the original substation structure maintains its safety during frequent earthquakes and wind loads. Upon encountering exceptionally strong earthquakes, the structure exhibited significantly increased lateral inter-story displacement angle. After reinforcement with BRB devices, the lateral inter-story displacement angle during rare seismic waves showed a 53% reduction relative to the unfortified structure, accompanied by a 13% decrease in base shear force. Under the 10-level wind load, the utmost lateral displacement diminished by 44%, and the peak stress saw a 37.5% reduction. The inclusion of BRBs notably dissipates the energy of earthquakes and wind loads, which provides a reference for designing substations that withstand such external disaster conditions.

**Keywords:** Substation, Earthquake action, Wind load, Dynamic response, Buckling restrained brace

## 1 Introduction

Skid-mounted substations with electronic control are widely used in petrochemical projects because of their simple structure and convenient production. Due to the high center of gravity of the skid skeleton, these substations are highly sensitive to natural disasters such as earthquake and wind load, resulting in poor resistance. China is located in the Circum-Pacific seismic belt and the Eurasian seismic belt, and frequent earthquake disasters can easily cause damage to such structures. Exploring the durability of frame structures within skid-mounted, electronically controlled substations against seismic activity and strong winds is crucial. Zijiang Yang et al. [1] used mobile power

to enhance the seismic capacity of distribution systems. Jichao Li et al. [2] proposed a probability-based seismic resilience assessment method for substation systems. Hatziargyriou et al. [3] developed a reinforcement framework to boost the seismic performance of the power system. Huangbin Liang et al. [4] developed a simulation model for assessing the seismic vulnerability of substations using flow diagrams and state trees. Hao Tang et al. [5] studied the wind load characteristics and wind-induced responses of a 1000 kV UHV substation frame under different wind angles and terrain conditions. Xinyu Ouyang et al. [6] applied a performance-based plastic design method to conduct seismic fragility analysis of reinforced concrete frames strengthened by buckling-restrained brace. Xiao Liu et al. [7] proposed a method for rapid seismic risk assessment of substation based on minimum cut sets. However, the existing seismic and wind resistance analysis of substation steel frames is mainly aimed at the original structure, with limited studies on reinforced substations.

Regarding the substation's steel frame structure that fails to comply with or closely approaches the current seismic code requirements, the author proposes using buckling-restrained braces (BRBs) to strengthen and improve the seismic and wind resistance of the structure. In order to explore the dynamic response analysis of BRB-reinforced structures under high-intensity earthquakes and wind loads, this paper uses SAP2000 software to perform response spectral analysis and nonlinear time-domain analysis, and compares the performance parameters such as inter-story displacement angle and base shear forces. This study serves as a reference for the research of seismic and wind resistance of the substation.

## 2 Engineering Overview and Model

### 2.1 Project Profile

The skeleton structure of a skid-mounted, electronically controlled integrated substation is selected as the research object, which is welded by steel-integrated welding. The frame structure consists primarily of beams, columns, and plates, with dimensions of  $33.9 \times 4 \times 7.8$  m. The intensity of seismic fortification ranges from 8 degrees. The design earthquake group is the second group, the site category is II. The design frequent and rare earthquake accelerations are 0.07 g and 0.4 g, respectively. The site characteristic periods correspond to 0.4 s and 0.45 s, respectively. The roof dead load is 0.3 kN/m<sup>2</sup>, the roof live load is 0.5 kN/m<sup>2</sup>, and the wall dead load is 0.3 kN/m<sup>2</sup>. The main material selected was Q355 low-alloy high-strength structural steel, and the structural system was an ordinary rigid frame.

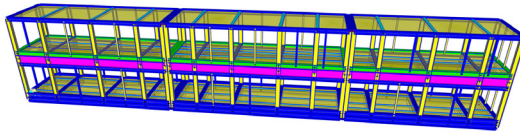
### 2.2 Finite Element Model

Fig. 1 shows the three-dimensional space model established by SAP2000 finite element software. Material mechanical parameters are listed in Table 1, and the thin-walled components such as the transformer shell, substation box, and walls are ignored. The transverse direction of the structure is parallel to the coordinate Y-axis, the longitudinal direction is parallel to the X-axis, and the column is parallel to the Z-axis. SAP2000 is

an object-oriented software based on finite element theory. For the steel frame mainly composed of beams and columns, linear elements are used without complex meshing, so the model is discretized into finite elements by the automatic subdivision function. The constraint condition of the model is that all the bottom column bases are hinged.

**Table 1.** Properties of materials pertinent to mechanical analysis in the calculations.

Steel materials	Elasticity modulus	Density	Tensile strength
Q355	206 GPa	7850 kg/m <sup>3</sup>	470 MPa



**Fig. 1.** Finite element model of the skid-mounted substation (SAP2000).

### 3 Seismic Response Spectrum Analysis

#### 3.1 Exertion of Seismic Action

China's seismic code requires that structures demonstrate different levels of resistance throughout their life cycle when subjected to various spectrums or magnitudes of seismic activity. According to the requirements of the National Standard of the People's Republic of China, "Code for Seismic Design of Power Facilities" GB50260-2013 [8], the seismic acceleration response spectrum for design purposes is identified, and the appropriate seismic wave is introduced. Because the substation is the main transfer link of the gathering and transportation system, a high-standard design is adopted to ensure an extremely high safety factor. Table 2 shows the basic parameters of the earthquake action.

**Table 2.** Basic parameters of seismic action.

Impact of earthquakes	Basic acceleration	Characteristic period/s	Maximum impact factor
Frequent intensity	0.07 g	0.40	0.16
Rare intensity	0.40 g	0.45	0.90

#### 3.2 Modal Analysis

Because the deformation and stress of the substation frame are related to the natural vibration period and vibration mode under dynamic loads such as earthquakes and wind, the modal analysis of the substation is conducted using SAP2000 software. Table 3 shows that the first 10 order vibration modes and response frequencies of the substation are obtained. Utilizing SAP2000 for modal analysis and calculation, the horizontal

fundamental natural frequency of the transfer station frame structure is 1.77 Hz. The first three modes are shown in Fig. 2.

**Table 3.** Top 10 order natural frequency table.

Order	1	2	3	4	5	6	7	8	9	10
Frequency/Hz	1.77	1.90	2.52	3.09	4.06	4.44	5.55	6.41	6.85	7.03

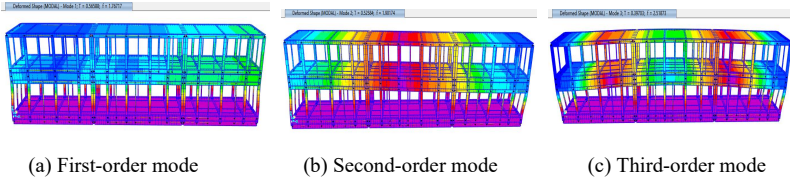


**Fig. 2.** Mode shape diagrams for the first three orders (SAP2000).

### 3.3 Results of Spectrum Analysis

#### Stress and Displacement Results.

The CQC method is used to integrate the frame structure's vibrational modes while factoring in the impact of random eccentricity. As shown in Fig. 3 and Fig. 4 that the maximum displacement occurs at the roof beam, and stress concentration occurs at the connection between the roof beam, the column and the foundation.

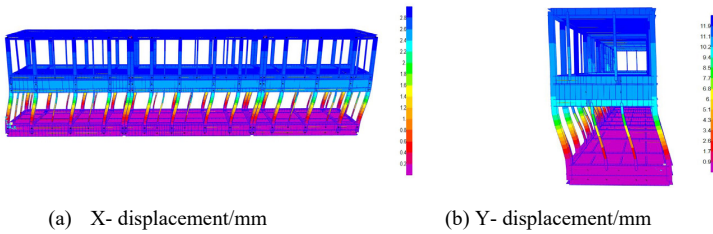


**Fig. 3.** The displacement nephogram in the X-axis and Y-axis directions (SAP2000).

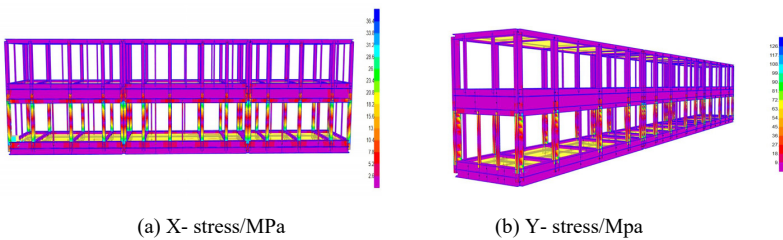


**Fig. 4.** The stress nephogram in the X-axis and Y-axis directions (SAP2000).

Table 4 reveals the peak stress on the framework reaches 126 MPa, which is less than the yield strength of the Q355 material, suggesting that the structure is within its elastic limit. Under the rare earthquake intensity, the peak stress is 840 MPa, which is significantly higher than the yield strength of 355 MPa. This indicates the onset of the yield phase during the rare earthquake intensity, thus calling for a nonlinear approach to analysis.

**Table 4.** The maximum displacement and stress of the structure under different intensities.

Impact of earthquake	Displacement /mm	Stress /MPa	Configuration status
Frequent intensity (X-axis)	2.8	36.4	Safety
Frequent intensity (Y-axis)	11.9	126	Safety
Rare intensity (X-axis)	16.8	210	Safety
Rare intensity (Y-axis)	77	840	Unsafety

**Inter-Story Displacement Angle.**

The vibration mode decomposition response spectrum method (CQC) is used to analyze the structure. Fig. 5 illustrates the inter-story displacement angles for the structure. Due to the large length-to-width ratio of the original structure, The angles of displacement between stories along the X-axis and Y-axis directions are greatly different. The maximum value under frequent intensity is 1/304, which does not exceed 1/250, satisfying the seismic design criterion of "undamaged under minor earthquakes". The peak displacement angle under regularly observed seismic events is 1/304, comfortably within the "no damage in minor quakes" safety threshold of 1/250. However, under rare seismic intensities, this angle reaches 1/49, breaching the "remain standing in major quakes" criterion (set at 1/50), thereby not conforming to particular safety standards regarding inter-story angles.

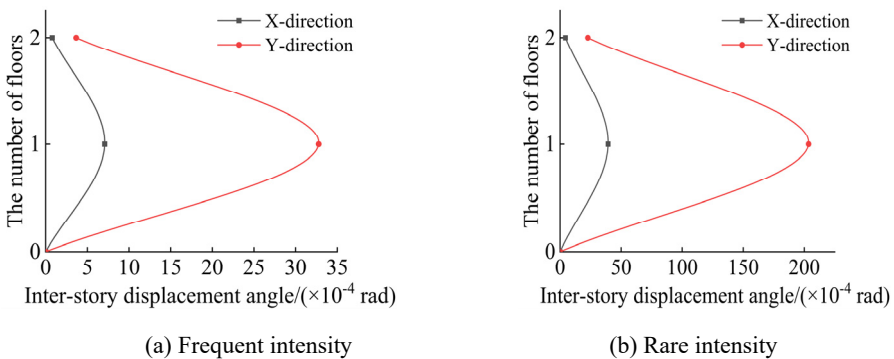
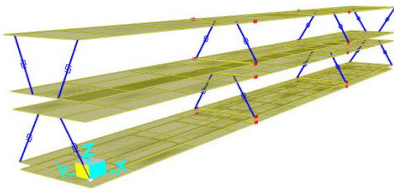


**Fig. 5.** Inter-story displacement angle(CQC).

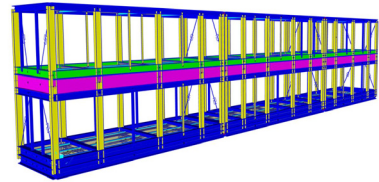
## 4 Buckling-Restrained Brace Structure

### 4.1 BRB Structure Layout

Because the inter-story position angle ( $1/49$ ) of the structure along the Y-axis direction exceeds the fortification safety value ( $1/50$ ) for a large earthquake, the buckling-restrained braces (BRBs) are arranged along the Y-axis direction of the structural coordinates. To avoid affecting the internal use of the substation and effectively reduce the displacement between the layers, the BRB components are arranged on the side of the substation structure and at  $1/3$  of the longitudinal side span. The layout is eccentric and X-type, layer by layer. The component model adopts the BRB200, and the layout orientation is shown in Fig. 6(a). In SAP2000, the Plastic (Wen) connection element is used to accurately simulate the buckling-restrained brace, in which the effective stiffness is  $50 \text{ kN/mm}$ , the post-yield stiffness coefficient is  $0.035$ , the yield index is  $5$ , the yield bearing capacity is  $200 \text{ kN}$ , the yield displacement is  $4 \text{ mm}$ , and the width and height of the external dimension are  $150 \times 150 \text{ mm}$ . Fig. 6(b) displays the three-dimensional overall model.



(a) Arrangement of BRB structure



(b) Integrated graph

**Fig. 6.** Integral and layout of finite element models of BRB-containing structures (SAP2000).

### 4.2 Modal Analysis

The first 10-order modal frequencies are shown in Fig. 7. In the original structure, the initial three modes include translation in the X direction, torsion, and translation in the Y direction. The first three periods are  $0.57 \text{ s}$ ,  $0.52 \text{ s}$  and  $0.40 \text{ s}$ . The second mode of the original structure is torsion, which indicates that the lateral stiffness of the structure along the two principal axes differ significantly, which will affect structural security. The modal analysis of the BRB structure shows that the first three modes are X-direction translation, Y-direction translation, and torsion, and the first three periods are  $0.42 \text{ s}$ ,  $0.37 \text{ s}$ , and  $0.31 \text{ s}$ , respectively. This indicates that adding a certain amount of buckling-restrained braces to the exterior and interior of the structure will increase its lateral displacement stiffness, preventing the first two vibration modes from entering torsion too early, and meet code requirements.

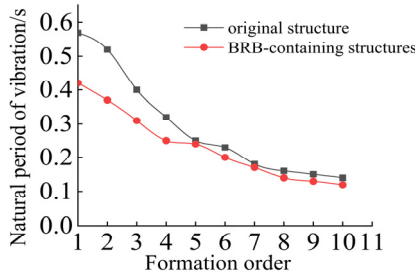


Fig. 7. Structural natural period.

## 5 Nonlinear Time History Analysis Under Rare Intensity

### 5.1 Selection of Seismic Wave

Because the period of the steel frame-buckling restrained brace structure is similar to that of the ordinary rigid frame structure, the same seismic wave can be selected as for the ordinary rigid frame structure. According to the "Code for Seismic Design of Buildings" (GB50011-2010) (2016 Edition) 5.1.2 [9], an artificial wave (RH2TG040 wave) and two natural waves (EL-Centro wave, Lanzhou wave) are selected for nonlinear time history analysis of the structure. Table 5 outlines the base shear force outcomes when subjected to three seismic waves. The base shear force for each individual wave is not less than 65% of the CQC method's calculation, while the mean base shear force derived from multiple waves is not less than 80% of the CQC method's findings. At the same time, the input calculation of each seismic wave is not more than 135%, and the average is not more than 120%. This indicates that the three seismic waves meet the requirements of the specification.

Table 5. Evaluation of the structure's foundational shear force during rare earthquakes.

Seismic wave	Along the Y-axis direction		Along the X-axis direction	
	Base shear (kN)	Ratio to response spectrum (%)	Base shear (kN)	Ratio to response spectrum (%)
CQC	2,718	/	3,327	/
RH2TG040	2,435	90	3,392	102
EL-Centro	2,994	110	3,118	94
Lanzhou	2,692	99	2,787	84
Average	2,707	99	3,099	93

### 5.2 Inter-Story Drift Angle of Rare Earthquake

Because the substation framework enters a plastic state under the rare earthquake, the structures before and after reinforcement underwent a nonlinear time-history analysis,

each subjected to the forces of a rare seismic wave. Table 6 illustrates the peak inter-layer displacement results for the original structure exposed to three types of seismic waves. The interlayer displacement along the Y-axis direction is more obvious than that in the X-axis direction, with the maximum value being 70.20 mm.

**Table 6.** The original structure's inter-story displacement under rare seismic wave.

Seismic wave	Along the Y-axis direction (mm)		Along the X-axis direction (mm)	
	First floor	Second floor	First floor	Second floor
EL-centro	70.20	7.86	14.22	1.58
Lanzhou	61.11	6.66	10.49	1.22
RH2TG040	56.38	6.24	11.68	1.38

Fig. 8 illustrates that the peak displacement angle between stories in the initial configuration reaches a ratio of 1/51. The buckling-restrained brace structure has the strongest energy dissipation capacity under the action of the EL-Centro wave, and the inter-story displacement angle is greatly reduced. At this time, the maximum value is 1/109, and the angular inter-story drift change curve becomes more gradual. The maximum values of the original structure and the BRB-containing structure does not exceed 1/50, which meets the fortification requirements of "no collapsing in strong earthquakes".

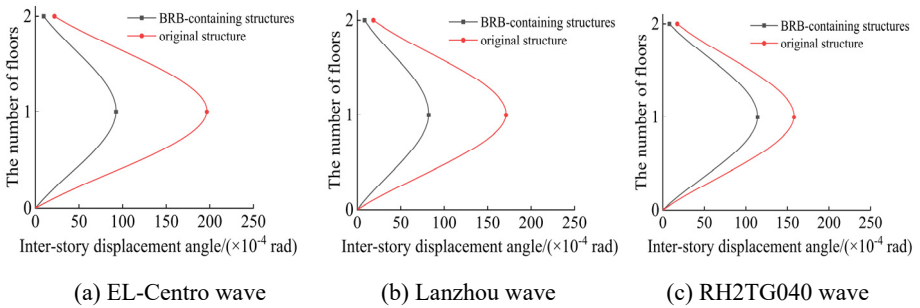


**Fig. 8.** Angular inter-story drift along the Y-axis direction.

Compared with the original structure, the supreme inter-story displacement angle along the Y-axis has diminished by 53%. The reinforced structure exhibits a 47% inter-story displacement ratio relative to the original structure, meeting the requirement that the lateral displacement ratio for the damping structure and the non-damping structure under rare earthquakes is less than 75%. This shows that buckling-restrained braces can significantly elevate the structure's capacity to absorb and dissipate seismic energy, contributing to enhanced safety.

### 5.3 Evolution of Base Shear Over Time

Base shear response over time for the initial structure and BRB-containing structure under the El-Centro wave during frequent and rare earthquakes is shown in Fig. 9. Fig. 9

outlines that the maximum value of the lateral base shear force of the original structure under rare earthquakes is  $2.99 \times 10^6$  kN, and the maximum value of the lateral base shear force of the structure under frequent earthquakes is  $5.24 \times 10^5$  kN with the ratio of 571%. Under rare seismic conditions, the maximum lateral base shear force recorded for the BRB-strengthened structure is  $2.62 \times 10^6$  kN. For frequent seismic occurrences, this value stands at  $4.78 \times 10^5$  kN, and the ratio of the two is 548%.

With the reinforcements, the building's overall lateral base shear force decreased by 13% compared to its original state. As demonstrated, the steel frame-buckling-restrained brace structure delays the time to enter the plastic stage under the action of rare earthquakes, and the base shear force of the structure decreases significantly.

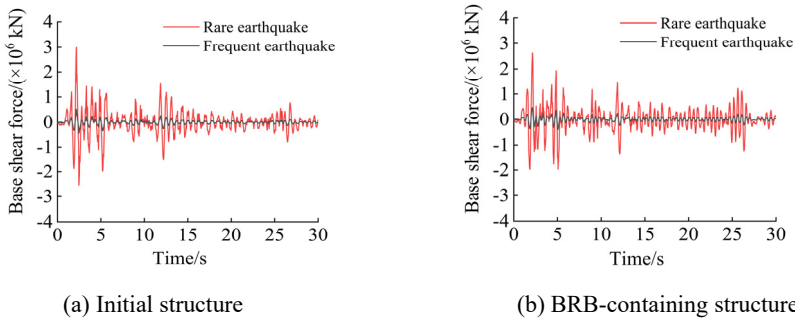


Fig. 9. Temporal variation of bottom shear force caused by El-Centro seismic wave.

### 5.4 Load-Deformation Hysteresis of BRBs

The performance in terms of energy absorption of the buckling-restrained brace (BRB) is depicted through its hysteresis curve. A buckling-restrained brace (BRB) positioned on the first floor is selected to investigate its hysteretic performance.

As shown in Fig. 10, the maximum deformation of the buckling-restrained brace under the rare earthquake EL-Centro seismic wave is 11.45 mm. The hysteretic curve of the buckling-restrained brace is well-developed, showing a spindle shape, indicating that the BRB possesses an effective energy absorption capability.

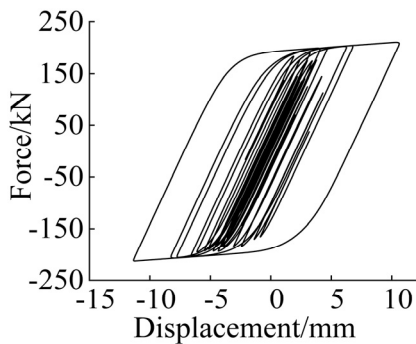


Fig. 10. Hysteresis curve of buckling restrained brace.

## 6 Application of Wind Force

Due to the influence of typhoons in China's coastal areas, wind disasters with winds exceeding level 10 often occur. Under the action of pressure difference, the air flows to form wind, and its strength is generally determined by wind pressure. The relationship between wind speed and wind pressure can be expressed by the Bernoulli equation in fluid mechanics [10]:

$$\omega = \frac{1}{2}\rho v^2 = \frac{1}{2} \frac{\gamma}{g} v^2 \tag{1}$$

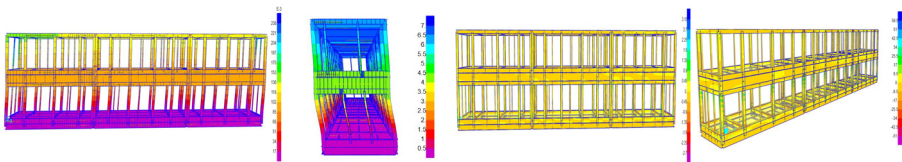
In the formula:  $w$  is the wind pressure per unit area,  $\text{kN/m}^2$ ;  $\rho$  is air density,  $\text{t/m}^3$ ;  $v$  is wind speed,  $\text{m/s}$ ;  $\gamma$  is mass per unit volume,  $\text{kN/m}^3$ ;  $g$  denotes gravitational acceleration,  $\text{m/s}^2$ . Wind load belongs to surface loads. In this model, we assumed a wind velocity of  $30 \text{ m/s}$ , ground-level wind pressure of  $0.56 \text{ kN/m}^2$ , along with standard coefficients for shape and layer height variations, both set at  $1.0$ .

The wind load is directional, so the wind resistance of the four windward surfaces is analyzed in SAP2000, which are along the X, -X, Y, and -Y axis directions. The wind load is calculated automatically by SAP2000. Since the wind action surface comes from the rigid partition range, a quasi-rigid partition is defined for each floor slab and bound to each different elevation.

### 6.1 Analysis of Wind Load Response

#### Stress and Displacement Results.

Fig. 11 illustrates that the frame's top is where the maximum displacement occurs, and the stress concentration occurs at the connection of the beam, column and foundation of the frame. Table 7 shows the total displacement and stress response of the original structure of the substation frame in four directions.



(a) X- displacement/mm (b) Y- displacement/mm (c) X- stress/MPa (d) Y- stress/Mpa

**Fig. 11.** Displacement and stress cloud diagrams for the initial structure under the positive Y-directed wind load (SAP2000).

**Table 7.** Response of the initial structure to wind forces in four orientations.

Wind load direction	Maximum displacement/mm	Maximum stress/MPa	Configuration status
The positive X direction	0.238	3.15	Safety

The negative X direction	0.308	3.85	Safety
The positive Y direction	7.0	59.5	Safety
The negative Y direction	6.3	52.5	Safety

The corresponding safety factors are 149.21, 122.08, 7.90 and 8.95 respectively, which are greater than the minimum value of 2.5 allowed by the specification. It signals that even under a level 10 wind load, the structure would remain intact.

The electrical equipment in the substation is highly sensitive to vibration. Fig. 12 depicts the maximal displacement reached by the structure under Y-direction wind load after installing the BRB on the lateral surface is 3.92 mm, which is 44% lower than that of the original structure, and the peak stress dropped by 37.5%, settling at 35 MPa. By reducing the maximum stress on the structure through reinforcement, structural deformation is minimized, thereby mitigating the vibration effects on the equipment and ensuring its stable operation.

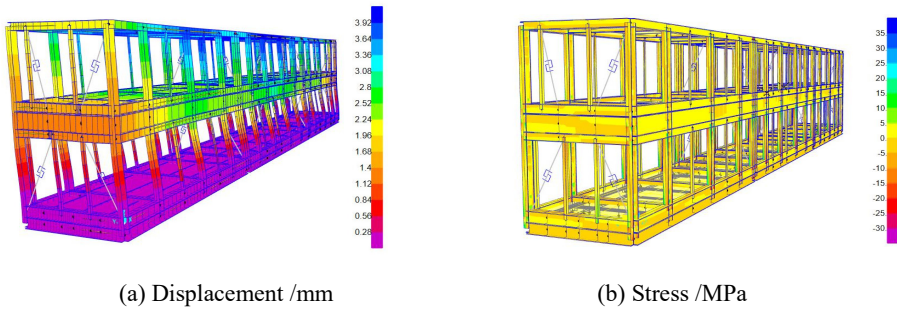


**Fig. 12.** Displacement and stress cloud diagrams for BRB-fortified structure under the positive Y-directed wind load (SAP2000).

**Interlayer Displacement and Shear Force.**

If the electrical equipment within the substation fails due to excessive displacement, it may lead to fire hazards or other safety incidents. Reducing the inter-story displacement minimizes the risk of damage to electrical equipment from structural movements and ensures their proper functioning. Fig. 13 illustrates that, when subjected to a wind load of intensity level 10, the peak inter-story displacement of the strengthened structure is diminished by 57.3%, and the peak inter-story shear force of the initial structure is decreased from 219 kN to 214 kN. It is shown that the BRB structure effectively dissipates wind load energy and significantly reduces interlayer displacement.

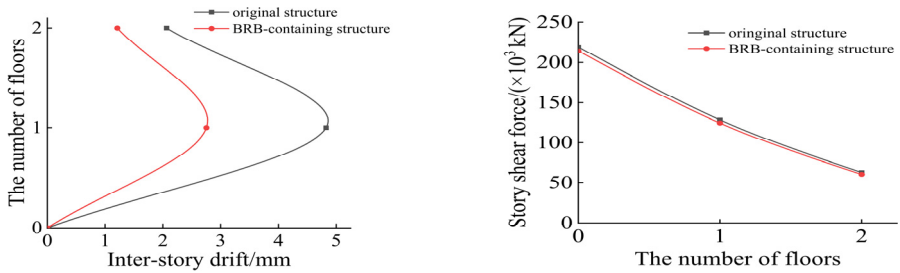


**Fig. 13.** Interlayer displacement and shear force for structures under the positive Y-directed wind load.

## 7 Conclusion

Supported by the numerical simulation of the seismic and wind resistance before and after the reinforcement of the substation, the conclusions below can be derived:

(1) Under the rare intensity, the lateral inter-story drift angle of the substation's framework was reduced by over half, and the base shear force decreased by 13% after the BRB reinforcement. Upon encountering the three rare seismic waves of EL-Centro, Lanzhou and RH2TG040, the reductions in the structure's lateral inter-story displacement angles were 53%, 52%, and 27.8%, respectively. The BRB structure produced large yield deformation, effectively dissipated seismic energy, and improved the structural response to seismic activity.

(2) Upon encountering a 10-level wind load, the structure's peak stress in the Y-axis direction after the installation of BRB was reduced by 37.5% relative to the initial structure, and the peak Interlayer displacement dropped by 57.3%, which effectively dissipated the wind load energy and improved the wind resistance of the substation framework.

(3) With regard to the substation frame structure with a high length-width ratio, BRBs can be used to reinforce the side span and middle span of the structure with the aim of significantly improving the stability of the structure, which is helpful for safer design in areas with active earthquakes and wind loads.

## Reference

1. Yang, Z., Dehghanian, P., & Nazemi, M. (2019). Enhancing Seismic Resilience of Electric Power Distribution Systems with Mobile Power Sources [J]. 2019 IEEE Industry Applications Society Annual Meeting, 16, no.1,1-7.
2. Ji-chao Li, Qingxue S., Tao Wang. (2020). Probability-based seismic resilience assessment method for substation systems [J]. Structure and Infrastructure Engineering, 79,no.4, 71-83.
3. Hatziairyriou, M. H. O. M. N. T. D. (2020).A Systematic Method for Power System Hardening to Increase Resilience Against Earthquakes [J]. IEEE Systems Journal,15,no.4,4970-4979.

4. Xie, H. L. (2021). System Vulnerability Analysis Simulation Model for Substation Subjected to Earthquakes [J]. *IEEE Transactions on Power Delivery*, 37,no.4, 2684–2692.
5. Tang, H., Li, F., Zhi, X., & Zhao, J. (2024). Wind load characteristics and effects of 1000kV UHV substation frame based on HFFB [J]. *Wind and Structures*, 38(6), 477–492.
6. Xinyu Ouyang. Seismic fragility analysis of buckling-restrained brace-strengthened reinforced concrete frames using a performance-based plastic design method [J]. *Structures*, 2022,43: Pages 338-350.
7. Xiao Liu, &nbsp;Wang Z., &nbsp;Qiang Xie. (2024). Rapid assessment of substation earthquake risk based on minimal cut sets [J]. *Electric Power Systems Research*, 229, Article 110175.
8. General Administration of Quality Supervision, Inspection and Quarantine of the People's Republic of China, et al. *Seismic Design Code for Power Facilities. GB 50260-2013* [S], China Standards Press, 2013.
9. General Administration of Quality Supervision, Inspection and Quarantine of the People's Republic of China, et al. *Building Seismic Design Code: GB 50011-2010* [S]. 2016 ed., China Architecture & Building Press, 2016.
10. Totokoja, J., (PhD), S. R., (PhD), J. L. D., Nabende, A., & Nagulama, M. (2023). Optimization of The Vertical Axis Wind Turbine For Localization In Low Wind Speed Areas [J]. *International Journal of Progressive Sciences and Technologies*, 17,no.1, 0.

**Open Access** This chapter is licensed under the terms of the Creative Commons Attribution-NonCommercial 4.0 International License (<http://creativecommons.org/licenses/by-nc/4.0/>), which permits any noncommercial use, sharing, adaptation, distribution and reproduction in any medium or format, as long as you give appropriate credit to the original author(s) and the source, provide a link to the Creative Commons license and indicate if changes were made.

The images or other third party material in this chapter are included in the chapter's Creative Commons license, unless indicated otherwise in a credit line to the material. If material is not included in the chapter's Creative Commons license and your intended use is not permitted by statutory regulation or exceeds the permitted use, you will need to obtain permission directly from the copyright holder.

